ELSEVIER

Marine Geology 241 (2007) 33–43

MARINE GEOLOGY
INTERNATIONAL JOURNAL OF MARINE GEOLOGY, GEOCHEMISTRY AND GEOPHYSICS

www.elsevier.com/locate/margeo

High-resolution, deep tow, multichannel seismic and sidescan sonar survey of the submarine mounds and associated BSR off Nicaragua pacific margin

A.R. Talukder [a,*], J. Bialas [a], D. Klaeschen [a], D. Buerk [a], W. Brueckmann [a], T. Reston [a], M. Breitzke [b]

[a] *IFM-GEOMAR Research Center for Marine ScienceWischhofstr. 1-324148 Kiel, Germany*
[b] *Alfred-Wegener-Institute for Polar and Marine Research Columbusstr. 27568 Bremerhaven, Germany*

Received 2 May 2006; received in revised form 9 February 2007; accepted 2 March 2007

Abstract

Bathymetric and conventional multichannel seismic surveys offshore Nicaragua and Costa Rica have revealed numerous mud mounds beneath which the generally widespread BSR is not well imaged. However, many of the mounds are partially capped by patches of authigenic carbonate crusts, so it was not clear if the semitransparent seismic facies and the apparent gaps in the BSR beneath the mounds are real or due to poor normal-incidence seismic penetration through the cap rocks. To address these problems, a high-resolution seismic survey was carried out over the continental slope of the Nicaraguan Pacific margin using a deep towed multichannel seismic streamer (DTMCS) along with a sidescan sonar system (DTS) to image submarine mud mounds and the associated BSR. The proximity of the very short (39 m active length) but high-resolution 17 channel streamer to the seafloor of the deep towed system allows greatly improved lateral resolution whereas the relatively large source–receiver offset allows the undershooting of the cap rocks. For the first time our data show that the BSR in many cases continues but rises beneath the mounds. This is consistent with the advection of deep warm fluids and thus increased heat flow through the mounds. The occurrence of mud mounds seems to be controlled by the locations of faults.
© 2007 Elsevier B.V. All rights reserved.

Keywords: mud mounds; gas hydrate; BSR; Nicaragua; erosive margin

1. Introduction

It has long been considered that the sedimentary dynamics in the continental margins mainly depends on external factors such as relative sea level changes and sediment supply. However, recently the importance of the subsurface fluid flows and mud mobilization in shaping the margins is being understood. Recent discoveries show that submarine mud volcanoes, mud diapirs and/or other fluid venting structures are global, numerous and exist in all tectonic contexts, although the majority of them is located in the convergent margins (Kopf, 2002). All these areas have at least one common characteristic, which is the existence of an overpressured source layer in the sedimentary

* Corresponding author. Tel.: +49 431 6002320.
E-mail addresses: atalukder@ifm-geomar.de (A.R. Talukder), jbialas@ifm-geomar.de (J. Bialas), dklaeschen@ifm-geomar.de (D. Klaeschen), dbuerk@ifm-geomar.de (D. Buerk), wbrueckmann@ifm-geomar.de (W. Brueckmann), treston@ifm-geomar.de (T. Reston), mbreitzke@awi-bremerhaven.de (M. Breitzke).

0025-3227/$ - see front matter © 2007 Elsevier B.V. All rights reserved.
doi:10.1016/j.margeo.2007.03.002

pile (Dimitrov, 2002). The primary cause of overpressure generation is rapid sedimentation. During sediment burials pore water is expelled by compaction and pore pressure increases with depth according to hydrostatic gradient. If sediment burial is rapid due to high sedimentation or tectonic loading, pore water cannot be expelled. These entrapped pore waters then produce overpressure, which inhibits any further mechanical compaction. Nevertheless, the overpressure produced by rapid sedimentation alone, with subsequent burial, rises generally as fast as lithostatic pressure (Osborne and Swarbrick, 1997), therefore, it is rarely sufficient to initiate mud diapirism, which needs to pierce the overburden (Jackson and Vendeville, 1994). Hence, the trigger mechanism of mud diapirism and volcanism needs additional factors such as faulting, increased fluid volume caused by hydrocarbon maturation etc. All these are related to regional geology. Mud volcanoes are different in their deep structures in different tectonic settings. In a comparative study between the mud volcanoes in Black Sea and in Mediterranean Ridge, Ivanov et al. (1996) suggest that the morphological differences between these two groups are due to their development in two different tectonic contexts. Thus the complete understanding of the trigger mechanism and its evolution in a particular region is very important to decipher the subsurface fluid regime, sediment dewatering and tectonic development of the area. Often, submarine mud volcanoes and mud diapirs are associated with gas hydrates that form at low temperature and high pressure conditions common in marine sediments. The base of gas hydrate is seismically characterized by a typical bottom simulating reflector (BSR) (Holbrook et al., 1996). The aim of this paper is to establish the trigger mechanism, and the factors controlling the distribution of the mud mounds and associated BSR in the Pacific margin offshore Nicaragua.

Bathymetric and conventional multichannel seismic surveys offshore Nicaragua and Costa Rica have revealed numerous mud mounds beneath which, the generally widespread BSR is not imaged. In general, the collective term “mound” is used, because it is difficult to clearly categorize these structures as mud volcanoes, mud diapirs or any other type of mud extrusion feature. Many of these mud mounds are partially capped by the patches of authigenic carbonate crusts, (Moerz et al., 2005) which inhibit the penetration of seismic energy. As a result, it was not clear if the semitransparent seismic facies and the apparent absence of BSR beneath the mounds are real or due to seismic imaging difficulties beneath the cap rocks. To overcome this problem, a deep towed multichannel seismic (DTMCS) as well as sidescan sonar (DTS) survey was carried out in the framework of SFB574 (Cooperative Research Project Volatiles and Fluids in Subduction Zones) during the *RV Sonne* Cruise SO173-1 in 2003 on the continental slope off Nicaragua’s Pacific coast (Fig. 1). In total 13 NW–SE striking profiles running parallel to the continental slope were recorded in water depths between 1000 to 2500 m.

2. Geological background

The Pacific margin off Costa Rica and Nicaragua is considered to be an erosive margin, where late Oligocene to early Miocene oceanic crust of the Cocos plate undergoes rapid subduction (DeMets et al., 1994) along the Middle America Trench (Ranero and von Huene, 2000). Results from ODP Drilling (Leg 170) indicate that the frontal wedge of the overriding plate, covered by 0.5–1.5 km of slope sediments, is of non-accretionary origin and characterized by a small frontal sediment prism of reworked slope sediments (Kimura et al., 1997; Ranero et al., 2000). A ca. 400 m thick sedimentary succession is underthrusting the igneous forearc wedge (Kimura et al., 1997; von Huene et al., 2004). Enigmatic low heat flow of 8–14 mW/m^2 was detected offshore Nicoya Peninsula along the drilling transect of Ocean Drilling Program (ODP) leg 170 and leg 205, which is six times lower than what would be expected from the sediment covering the crust of this age (Langseth and Silver, 1996; Silver et al., 2000). Unusual effective hydrothermal cooling is envisaged as explanation for the low temperature crust, most likely via advection of heat by fluid flow through abundant faults produced probably from bending of the down going slab. However, recent surveys and works suggest that the thermal state of the incoming plate changes parallel to the trench axis with higher heat flow to the NW of Nicoya Peninsula (Fisher et al., 2003; Grevemeyer et al., 2004, 2005). In the forearc, the heat flow seems to recover rapidly from depressed geotherms due to hydrothermal mining of heat in the incoming plate to conductive values as the circulation system is shut off by the overlying margin wedge (Grevemeyer et al., 2004, 2005).

Mud diapirs have been known in offshore Costa Rica from the first 3D seismic reflection data (Shipley et al., 1990, 1992). Further evidence for the fluid expulsion includes observations of vents and mud volcanoes with submersibles (Kahn et al., 1996; McAdoo et al., 1996). The most active fluid expulsion was observed at the large seaward most diapir and included authigenic carbonates, bacterial mats and chemoautotrophic communities

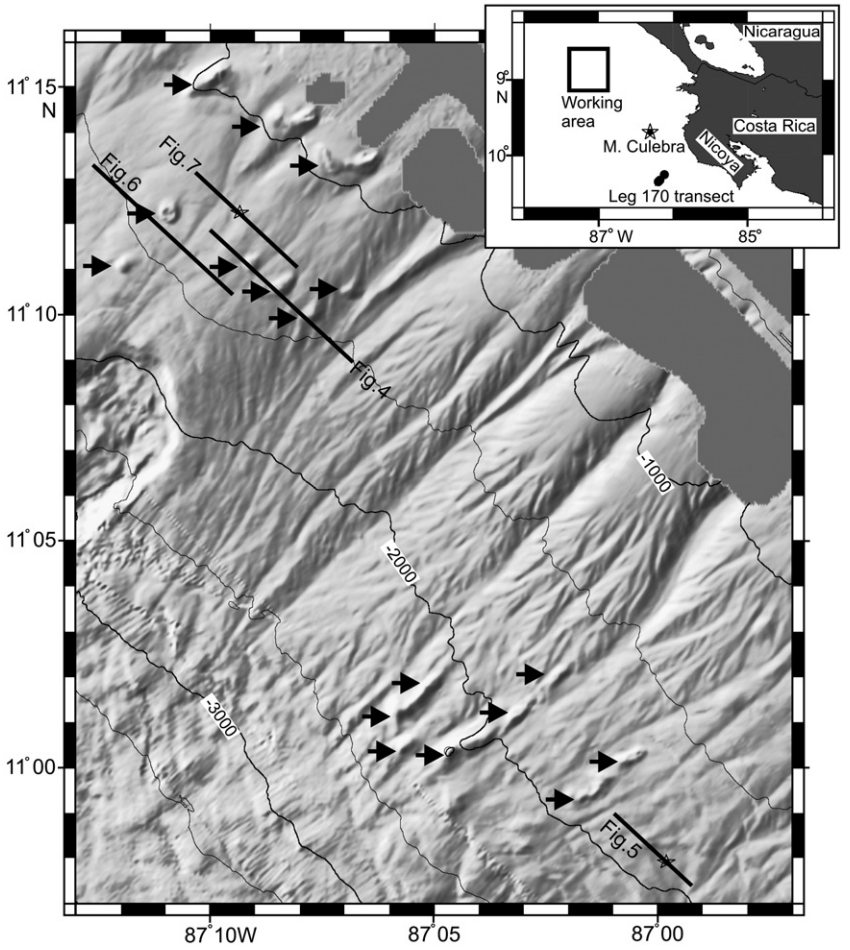

Fig. 1. Bathymetric relief map (illumination from NW) showing three main physiographic elements off Nicaragua pacific margin: submarine mud mounds (arrowed), deeply incised canyons and slide. Black lines refer the positions of Figs. 4–7. Star symbols indicate the mud mounds presented in their respective figures.

(Kahn et al., 1996). Later on numerous surveys off the Costa Rica and Nicaragua Margin have identified a variety of fluid expulsion features, including mound-like structures, as well as widespread and well-developed BSRs along the middle upper slope of much of the margin (Pecher et al., 1998; Bohrmann et al., 2002). Geologically, the mud mounds are underlain by deformed slope sediment, which rests in turn on the basement of the continental framework. Normal faulting has been imaged seismically across the midslope offshore Costa Rica and Nicaragua (Ranero and von Huene, 2000; MacIntosh et al., 2006) among which at least some of them are associated with mud mounds (Moerz et al., 2005). Dewatering mechanisms in the frontal prism, the deformed slope sediments, the underthrust sediments as well as gas hydrate processes are crucial to understand the tectonic development of the margin.

3. Methods

3.1. Deep towed seismic system (DTMCS) and sidescan sonar (DTS) lay out

The deep towed system of IFM-GEOMAR comprises a deep towed multichannel seismic streamer (DTMCS), a deep towed sidescan sonar (DTS) and a subbottom profiler (Fig. 2).

The sidescan sonar is an EdgeTech Full Spectrum dual frequency, chirp sidescan sonar system with 75 kHz and 410 kHz centre frequencies. In the 75 kHz mode the swath width imaged is 1500 m with a maximum across-track resolution of 5.6 cm. Working with 410 kHz sonar signals the swath width is 300 m with a maximum across-track resolution of 1.8 cm. Towing speed during surveys is usually between 2.0–3.0 kts, leading to an along-track resolution of 1.0–1.5 m. Therefore the resulting lines are

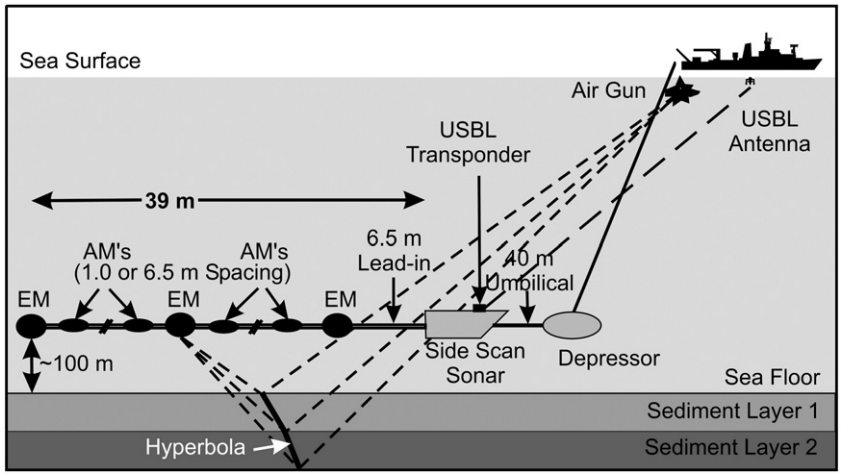

Fig. 2. Deep-towed multichannel seismic array (DTMCS) and sidescan sonar (DTS) configuration during the Cruise *RV Sonne* SO173-1 (2003). EM: engineering node; AM: acoustic node (modified from Breitzke and Bialas, 2003).

merged into a mosaic of 1 m pixel size for the 75 kHz mode and 0.25 m for the 410 kHz mode, surveyed at slower speed. Additionally the system contains a 2–16 kHz chirp subbottom profiler giving a nominal vertical resolution of approximately 10 cm and up to 50 m penetration. The maximum depth of deployment for the system is 6000 m. During the survey offshore Nicaragua, data were acquired in the 75 kHz mode.

The deep towed streamer was composed of 14 acoustic nodes (single hydrophone) and three engineering nodes (hydrophone plus depth and heading) (Breitzke and Bialas, 2003). Node spacing was either 1 or 6.5 m to allow a high-resolution imaging of subsurface structures by close subsurface reflection points. The position of the sidescan sonar tow fish was determined by the USBL (Ultra-short-base-line) positioning system POSIDONIA, which together with the engineering data of the streamer and the GPS data from the ship's antenna allows a precise (1% of the range) geometry processing of the deep tow seismic data for subsequent multichannel seismic data processing. As seismic source, a GI-Gun of 1.7 l generator volume was used. Seismic events were observed between 50–300 Hz. A towing depth of ca. 100 m above seafloor provided data with a lateral resolution that is ca. 3–4 times higher in 1000–2300 m water depth than can be achieved with a conventional surface streamer due to the reduction of the size of the Fresnel zone. The proximity of the streamer to the seafloor allowed also recording of wide angle reflection data with a very short multichannel streamer (39 m) and permitted imaging beneath the cap rocks.

Due to the hybrid nature of the seismic system (deep towed receiver, airgun source at the surface; Breitzke and Bialas, 2003), the standard CMP concept and processing could not be applied to this data set. Primarily from the recorded DGPS (Differential GPS), USBL and engineering data, the varying spatial locations and immersion depth of each hydrophone at each shot were calculated. After application of a band pass filter (90 Hz to 300 Hz), an amplitude preserved Kirchhoff 3D prestack-time migration was computed which considers all multichannel data with respect to the common reflection points for the target profile. The time migration image was computed with 2 m trace distance using a constant velocity of 1500 m/s.

4. Results

The continental margin off Nicaragua is dominated by deeply incised canyons and numerous mud mounds, as well as slides at the lower slope in the NE part of the survey area (Fig. 1).

4.1. Surface expression of mud mounds

The morphology of the mounds on the sea bottom has been analysed on deep tow sidescan sonar (DTS) images. Mud mounds are observed as circular or semicircular features with irregular boundaries and, in general, high-backscatter intensity compared with the general level of background backscatter intensity (Fig. 3). The stronger backscatter intensity can be caused by an irregular relief of the mound structures covered by patches of authigenic carbonate crust.

Mounds Buho and Hormiga are dome- or knoll-like mounds with a nearly circular, slightly elongated base and

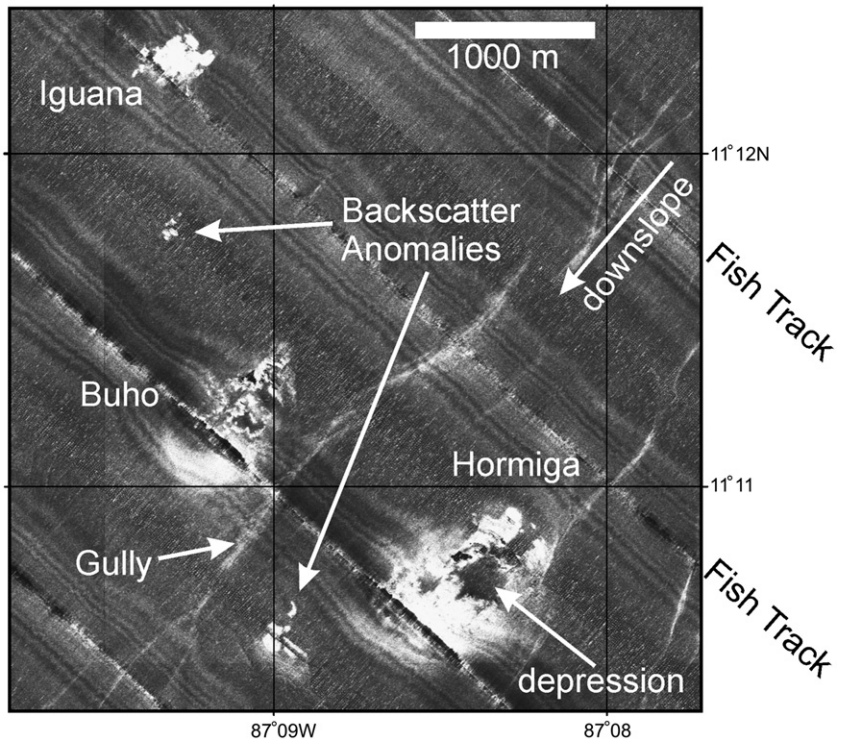

Fig. 3. Deep tow sidescan sonar (DTS) image of mounds Buho, Hormiga and Iguana characterized by high back scatter intensity (in white colour) compared with the general level of back ground scatter intensity.

steep downslope and flat upslope flanks (Fig. 3). They are located in about 1260 m water depth. The dome-shaped Mound Buho has a size of ca. 900 m × 700 m and a height of 40 m. The flat top area and the upslope side show a patchy high-backscatter intensity in the sidescan sonar image interpreted as outcropping authigenic carbonates with darker areas in between interpreted as slight depressions covered by hemipelagic seafloor sediment or shadows. It is remarkable that the steep SW flank of Mound Buho shows uniform high-backscatter intensity even when illuminated downslope from the fish track (Fig. 3). It can only be assumed that a more consolidated seafloor or a harder reflector under the hemipelagic sediment observed in this section with video ground truthing are responsible for the increased amplitude values. In the SE a somewhat chaotic structure of the sediments is interpreted as channel fill sediments.

The morphology of Mound Hormiga shows two flat summits separated through a small depression less than 5 m deep (Fig. 3). The size is ca. 1100 m × 850 m with a height of 60 m. In the sidescan sonar image the central depression shows uniform grey values interpreted as hemipelagic sediment coverage, surrounded by a patchy backscatter pattern which is probably caused by blocky carbonates resulting in bright backscatter and dark shadows. In the subbottom profile the contact between the mound facies and the adjacent channel deposits is not clearly imaged. Video observations on both mounds show only very sparse live vent fauna such as scattered clamshells (Sahling et al., 2003).

Mound Iguana shows very little topographic relief. It is situated on the shoulder of a canyon in about 1215 m water depth (Fig. 3). The size is approximately 380 m × 480 m and the elevation reaches just 25 m. In the high-resolution sidescan sonar data it is imaged with a very bright and uniform backscatter signal, bordered irregularly to the surrounding normal amplitude seafloor values and resembles therefore a high-backscatter patch (Fig. 3). Along the southwestern and southern border of the mound structure massive authigenic carbonates and abundant vent fauna (mytilid mussels and pogonophoran tubeworms) in cracks and fractures have been observed with video ground truthing. Bacterial mats have been observed in the sediments covering these cracks and fractures (Sahling et al., 2003). Further to the northeast more and more hemipelagic sediments cover the mound, still showing very bright backscatter in the sidescan image. This can be due to the penetration of the sonar

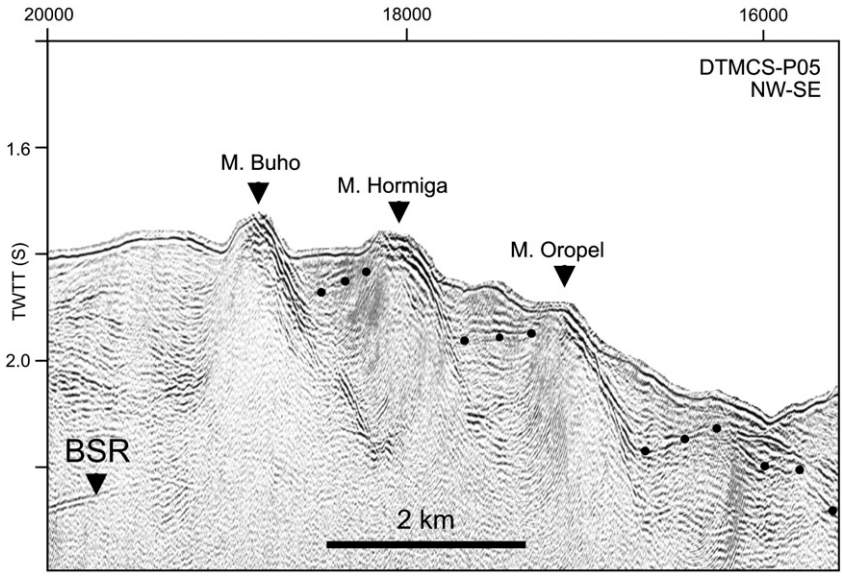

Fig. 4. Seismic interpretation of profile DTMCS-P05 (see the location in Fig. 1). Note that the mounds are associated with a vertical offset of the seafloor and sedimentary wedges (indicated by black dots) suggesting asymmetric growth. The strong inclined reflectors masking the SE side of the mound walls are artefacts produced by the asymmetric geometry of the deep-tow reflection system.

signal into the sediment and scattering at burrowed carbonates or volume scattering at mud clasts distributed in the sediment.

4.2. Occurrence of mud mounds and BSR

The mud mounds are of different sizes and most of them built positive topographic expression (up to ca. 130 m) above the surrounding seafloor. They are characterized by transparent or semitransparent seismic facies in the diapir like feeder structures tapering upward to cone shape geometry. In order to understand the trigger mechanism and evolution of the mud diapirism and/or volcanism, the geometrical relations between the feeder structures and country rocks have been analysed (Van Rensbegen et al., 1999). Although the profiles are margin parallel, the bathymetry changes from one side of the mound to the other. On the deeper side, in the marginal troughs, sedimentary strata produce wedge shape geometry fanning towards the feeder structures, which suggests that the material ascent was accompanied by normal faulting with the deeper side being downthrown (Fig. 4). In some marginal troughs, although in the lower part of the same sections reflectors are divergent toward the feeder structures, the uppermost reflectors are convergent toward the same indicating a forceful intrusion of the mud and fluid, apparently without being induced by faults (Fig. 5). This implies that the material ascents were initially triggered by a growth fault (Talukder et al., 2003). Analogue modelling of the diapir evolution suggests that during diapir rise, initially induced by faults, buoyant stresses in diapir increase as the overburden thins by faulting and the diapir grows. Driven by the fluid pressure the diapir eventually starts piercing as a forceful intrusion and continues growing even though the faulting has stopped (Vendeville and Jackson, 1992; Van Rensbegen et al., 1999). The angular unconformities found near some feeder structures

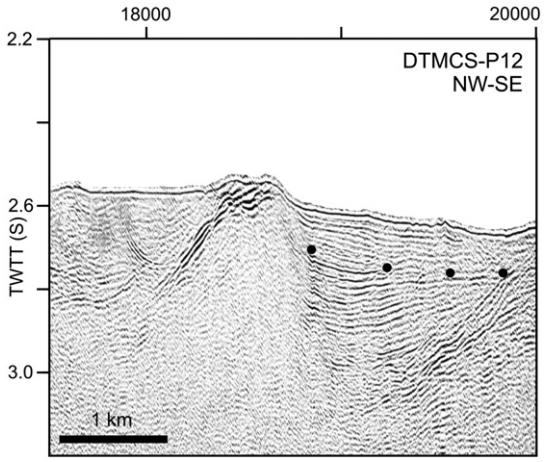

Fig. 5. Seismic interpretation of profile DTMCS-P12 (see the location in Fig. 1). Black dots indicate the upward transition from diverging to converging geometry of the reflector towards the mounds feeder structure.

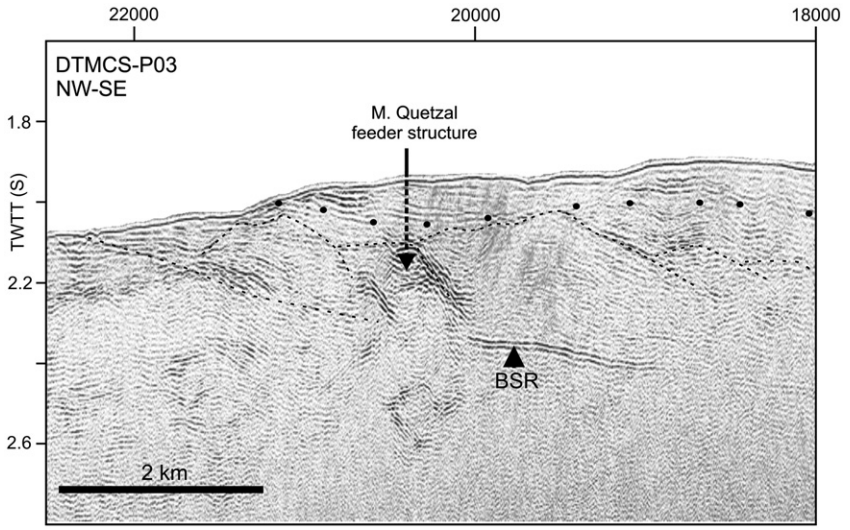

Fig. 6. Seismic interpretation of profile DTMCS-P03 (see the location in Fig. 1). Dotted lines and black dots indicate the tilted blocks and overlying unconformity respectively. The mound feeder structure is associated with a fault system, which seems to detach at the BSR level and the BSR seems to disappear where the fault connects the current seafloor.

become apparent conformities away from them. These local unconformities were most probably induced by the differential activation of diapirism and/or volcanism between two adjacent mounds and/or by their episodic activations. While some places fluids and muds stopped their ascent and remain buried at depth, others continued up to the seafloor producing mud mounds on it. Mud mounds on the seafloor as well as those buried beneath it form two distinct lineaments, subparallel (NW–SE) or perpendicular (NE–SW) to the bathymetric contours in the area (Fig. 1), which may correspond to the frontal and lateral ramp of the normal faults. Faulting is not synchronous throughout the whole area. While in some lines, faults are buried (Fig. 6), in other lines, they have produced offset on the seafloor (Fig. 4).

Our interpretation of the BSR in the area is based on three characteristics: i) its reverse polarity relative to the seafloor reflector ii) its cross-cutting relationship with the sedimentary stratigraphy and iii) it roughly parallels the sea bottom topography. The BSR is variable along the seismic lines in our used frequency windows (90–300 Hz), having high to moderate amplitudes near the mud mound feeder structures and seems to fade away from them. Furthermore, directly beneath the mounds, the BSR either rises (with or without considerable drop in amplitude) or seems to disappear. Based on the relation between the mounds and associated BSRs two groups of mounds have been found: i) BSR seems to disappear beneath the mounds (Fig. 4); ii) BSR is bent upward through the feeder structures beneath the mounds with or without considerable loss of the amplitudes (Fig. 7). For the 2nd group, no vertical offset on the seafloor from one side to another of the mound is observed, suggesting that these mud mounds may not be associated with current seafloor connecting faults (Fig. 7). In the line DTMCS-P03 a complex image of the BSR, mud mound feeder structure and faults is observed (Fig. 6). This line crosses through the SW flank of the mound Quetzal. On the SE side of the feeder structure, a typical BSR with clear negative polarity shows high amplitude near the mound and fades away from it. The mound is associated with a fault system, which seems to detach at the level of the BSR (Fig. 6). On NW side of the

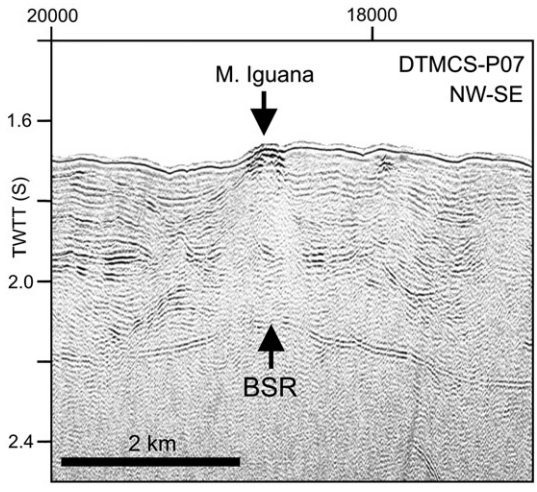

Fig. 7. Seismic interpretation of profile DTMCS-P07 (see the location in Fig. 1). The BSR is clearly imaged beneath the mound.

feeder structure, the BSR seems to disappear where the fault connects the current seafloor.

4.3. Temperature at the BSR depth

The experimental model for the methane hydrate stability conditions in seawater established by Dickens and Quinby-Hunt (1994) is used to estimate the temperature at the BSR depth. In this model the BSR depth is normalized with respect to the sea surface. In the study area, the maximum and minimum BSR depth vary between 1170 and 2204 mbss (m below sea surface), which correspond to the temperature from 13.8 °C to 18.48 °C. In a comparative study between the predicted temperature at BSR depth for seawater condition and the temperatures measured downhole from ten ODP drilling sites in both active and passive margins, Grevemeyer and Villiner (2001) show that in seven sites, the observed values are 1–2 degrees lower, while in others, 1–2 degrees higher. The temperature at the depth of the BSR marking the base of the gas hydrate stability zone in equilibrium condition, can be several degrees cooler than the theoretical values due to capillary effect (Ruppel, 1997). The capillary forces in fine grain sediments due to very small pore size may inhibit gas hydrate formation (Buffett, 2000). Theoretical calculation (Clennell et al., 1999) and laboratory measurements (Handa and Stupin, 1992; Zakrzewski and Handa, 1993) indicate that capillary forces in fine grained materials may depress dissociation temperatures by 0.5–8 °C. On the other hand the chemical impurities, for example small amount of ethane, carbon dioxide, hydrogen sulphide and higher hydrocarbons, can increase the temperature (Clennell et al., 1999).

The temperatures at BSR depths in some locations have been calculated using measured data from the existing few heat flow and CTD stations in the working area in order to compare them with the estimated values. The temperature at BSR depth is equal to the thermal gradient multiplied by the BSR depth below seafloor plus the temperature at the sea bottom. The nearest heat flow station H0201 (Cruise M54-2, 2002) is located ca. 22 km NW to the mound Iguana (Grevemeyer et al., 2005). The temperature at the sea bottom is derived from three Conductivity Temperature Depth (CTD) measurements (Cruise SO173, 2002) on the top of mounds Iguana, Carablanca and Quetzal. These CTD profiles have recorded the data up to approximately 19 m (at mound Iguana site) to only few centimeters from the seafloor (at the Carablanca site) and suggest no temperature anomaly on the top of those mounds (Mau et al., 2003). Finally the depth of the BSR is calculated from the seismic profiles using an average P wave velocity of 1700 m/s obtained from the borehole data of the ODP leg 170 offshore Costa Rica (Kimura et al., 1997).

The thermal gradient from heat flow probes is 0.0282 °C m^{-}, the seafloor temperature at Iguana site (water depths 1218 to 1253 mbss) has been measured as 3.83 to 3.73 °C, while the depth of the BSR has been found in the deep towed seismic data to be 376 to 358 mbsf (meter below seafloor). The calculated temperatures at BSR depth are 14.43 to 13.83 °C at the mound Iguana site. The corresponding estimated temperatures at the site (Mound Iguana) are 15.69 to 15.8 °C, which suggest that the temperature at the BSR depth is 1–2 degrees cooler than the experimental values from Dickens and Quinby-Hunt (1994).

5. Discussion

Submarine mud volcanism and diapirism is a common process in all tectonic environments and is generally attributed to the presence of an overpressured source layer. The principal mechanism of overpressure generation is rapid sedimentary or tectonic loading due to high sedimentation rates, accretion or shortening (Milkov, 2000; Dimitrov, 2002). However the mechanisms of their formation in the erosive Central America convergent margin are not well understood.

Deep penetrating seismic data show that the sedimentary cover lying over the frontal margin wedge in the midcontinental slope offshore Nicaragua is ca. 1 km thick (Ranero et al., 2000). In order to generate an overpressured source layer produced by high sedimentation rate in a sedimentary pile of ca. 1 km thickness, the sedimentation rate should exceed 800 m/Ma (Osborne and Swarbrick, 1997). The age of the sedimentary cover of the midcontinental slope off Nicaragua ranges from late Miocene to Holocene (Ranero et al., 2000) and the current sedimentation rate calculated from tephrachronology is ca. 200 m/Ma (Kutterolf et al., 2004), which is too low to produce an overpressured source layer leading to an eventual subsurface sediment mobilization (Mann and MacKenzie, 1990). The Logging-while-drilling (LWD) data from ODP drilling (Leg 170) offshore Nicoya Peninsula, Costa Rica also suggest that the sedimentary apron overlying the wedge is normally compacted (Kimura et al., 1997). However, although the upper portion of the underthrust section is partially drained due to fluid escape mainly by faulting, the lower portion remains nearly undrained (Saffer, 2003). New geophysical, geochemical and structural data gathered during the 2002 and 2003 *RV METEOR* and *Sonne* cruises indicate that the fluids at a number of mud mounds on the Central

America margin come from deep sources (Hensen et al., 2004). In general, fluids are significantly depleted in chloride and other major elements relative to seawater, suggesting a general process of freshwater addition and thus a common source of the fluids. Geochemical analysis on the methane hydrate, chloride anomalies and heat flow modelling of the mounds offshore Costa Rica indicate deeply sourced fluids generated by clay dehydration near the decollement (Hensen et al., 2004; Grevemeyer et al., 2004; Schmidt et al., 2005). It is likely that offshore Nicaragua the same mechanism and fluid source is the driving mechanism for mound formation. Deeply cutting faults, identified in MCS lines (Ranero et al., 2000; MacIntosh et al., 2006) could provide the pathways for the fluid migrating through the margin wedge. We suggest that when these high pressure, low salinity fluids reach the less permeable slope sedimentary apron, they remobilize the deepest sediments as the diapir like feeder structures that form mounds where they reach the seafloor. Thus deep faults provide the principal control on the mud mound distribution in the area.

The reverse polarity relative to the seafloor reflector and the temperature interval from 13.8 °C to 18.48 °C (−1–2 °C) at the BSR depth suggest that the extensive occurrence of BSRs is caused by the existence of free gas beneath the hydrate stability field (Holbrook et al., 1996) in the area. The diagenesis related BSRs resulted from the positive acoustic impedance contrast between silicate rich sediments of the different diagenetic stages, opal A, opal CT and quartz, have the same polarity as the seafloor reflection as well as occur at the temperature interval from 35 to 50 °C. The gas hydrates are generally not stable above 25 °C. (Berndt et al., 2004). The distribution of the high to moderate amplitude BSR around the mud mounds in the working area may indicate the preferential build up of free gas in those locations, probably due to increased hydrate dissociation near sites of the focussed fluid flows and mud diapirism (Wood et al., 2002).

Seafloor observations by OFOS video sled during the Cruise SO173 suggest that fluid venting seem to be among the highest in mound Iguana (Sahling et al., 2003), where BSR is clearly imaged across the mound. In order to verify if the BSR imaged beneath the mound Iguana is not a side echo (e.g. from the BSR just off to the side of the mound), the horizontal resolution or the diameter of the Fresnel zone has been considered. The seismic line is 125 m off-centre of the mound and the radius of the Fresnel zone at the seafloor is 54 m. At the seafloor, the mound lies out of the Fresnel zone. However, the Fresnel diameter increases with the depth and the diameter of the feeder structure of Mound Iguana at the BSR depth is ca. 1247 m. At the BSR depth, the feeder structure lies inside the Fresnel zone, and therefore, it can be considered that the imaged BSR is present beneath the mound. Further, the upward bending of the BSRs beneath the mound cannot be due to velocity pull up caused by the higher velocity in the carbonate crust, as the deep tow system images by wide angle reflections (undershooting) and the reflecting rays do not penetrate through the higher velocity crust (see Fig. 2). Here it seems likely that the temperature anomaly produced by the fluid flows was not sufficient to destabilize the P–T condition for hydrate, but to deflect upward the isotherm imaged as uplifted BSR in the feeder structure, implying that the upwelling fluids are not particularly hot. This is consistent with both regional and local heat flow data: offshore Costa Rica the heat flow on Mound Culebra is only 10–20 mW/m^2 higher than the background heat flow values (Grevemeyer et al., 2004). In contrast, the mud volcanoes in Barbados Accretionary prism (Henry et al., 1996) and Hakon Mosby mud volcano (Eldholm et al., 1999) have heat flow values over 1000 mW/m^2 above the regional background. We suggest that the fluid flux off Central America may reflect also a lower fluid flux that offshore Barbados is for instance known to be particularly high.

Although the BSR is observed beneath Mound Iguana (Fig. 7), it is not observed beneath some others (Fig. 4). However, this is unlikely due to elevated temperatures (associated with higher fluid flow) moving the entire subsurface into the free gas field, as Iguana is one of the more active mounds. The apparent absence of the BSRs seems to be systematic and characterized by the mounds that are associated with the faults connecting current seafloor (e.g. Fig. 4). Thus, BSR may be disrupted by the escape of some methane into the hydrate stability zone along faults, reducing the local concentration of methane gas beneath the gas hydrate stability zone (Holbrook et al., 1996; Gorman et al., 2002). The migration of gas through gas hydrated stability field has been observed in many places. Finite element modelling of the gas chimneys through hydrate stability field in the Cascadia margin off the Coast of Vancouver Island, suggests that in areas of fluid and heat flux methane gas can exist well inside the regional hydrate stability zone due to local temperature anomaly near the site of focused fluid flow (Wood et al., 2002). Alternatively, the gas hydrate in the surrounding sediments may seal the fault walls such that the water supply is too low to transform all the gas into gas hydrate (Taylor et al., 2000). However, the apparent absence of the BSR could also be related to signal penetration problems not associated with the carbonate caps of the mounds. The general lack of deeper reflections

despite the presence of deeper sedimentary layers and top basement suggests that the BSR is at the imaging limit of the acoustic penetration.

6. Conclusion

1. A deep towed seismic system can image the deep structure capped by carbonate crust, and thus offers a very useful tool for the submarine mud mound and gas hydrate research.
2. Faults controlled the initial trigger and the distribution of the mud mounds and diapir like feeder structures in the offshore Nicaragua. Two distinct lineaments (NW–SE and NE–SW) of mud mounds may indicate the frontal and lateral ramps of the extensional faults.
3. The distribution of the high to moderate amplitude BSR around the mud mound feeder structures suggests focussed fluid flow. The BSR can be traced (and is deflected slightly upward) beneath some mounds. The implication is that the fluids in the mounds offshore Nicaragua are cooler than that of other margins, and perhaps indicating a lower fluid flux.

Acknowledgements

This work has been financially supported by the Deutsche Forschungsgemeinschaft within the collaborative research project SFB574 (contribution N° 105). The deep-tow streamer and sidescan sonar were developed within the projects INGGAS and OMEGA of the gas hydrate initiative of the GEOTECHNOLOGIEN program, financially supported by the German Ministry for Science, Research and Technology (BMBF). We thank the editor and reviewers for their very constructive criticisms. Furthermore, we thank Captain Kull and his crew for their efficient help during *RV Sonne* cruise SO173-1.

References

Berndt, C., Buenz, S., Clayton, T., Mienert, J., Saunders, M., 2004. Seismic character of bottom simulating reflectors: examples from the mid-Norwegian margin. Mar. Petrol. Geol. 21, 723–733.

Bohrmann, G., Heeschen, K., Jung, C., Weinrebe, W., Baranov, B., Cailleau, B., Heath, R., Huehnerbach, V., Hort, M., Masson, D., 2002. Widespread fluid expulsion along the seafloor of the Costa Rica convergent margin. Terra Nova 14, 69–79.

Breitzke, M., Bialas, J., 2003. A deep-towed multichannel seismic streamer for very high-resolution surveys in full ocean depth. Mar. Seism. 21, 59–64.

Buffett, B.A., 2000. Clathrate hydrates. Annu. Rev. Earth Planet. Sci. 28, 477–507.

Clennell, M.B., Hovland, M., Booth, J.S., Henry, P., Winters, W.J., 1999. Formation of natural gas hydrates in marine sediments; 1 conceptual model of gas hydrate growth conditioned by host sediment properties. J. Geophys. Res. 92, 495–520.

DeMets, C., Gordon, R.G., Argus, D.F., Stein, S., 1994. Effect of recent revisions to the geomagnetic reversal time scale on estimates of current plate motions. Geophys. Res. Lett. 21, 2191–2194.

Dickens, G.R., Quinby-Hunt, M.S., 1994. Methane hydrate stability in seawater. Geophys. Res. Lett. 21, 2115–2118.

Dimitrov, L.I., 2002. Mud volcanoes — the most important pathway for degassing deeply buried sediments. Earth-Sci. Rev. 59 (1–4), 49–76.

Eldholm, O., Sundvor, E., Vogt, P.R., Hjelstuen, B.O., Crane, K., Nilsen, A.K., Gladczenko, T.P., 1999. SW Barents Sea continental margin heat flow and Hakon Mosby volcano. Geo-Mar. Lett. 19, 29–37.

Fisher, A.T., Stein, C.A., Harris, R.N., Wang, K., Silver, E.A., Pfender, M., Hutnak, M., Cherkaoui, A., Bodzin, R., Villinger, H., 2003. Abrupt thermal transition reveals hydrothermal boundary and role of seamounts within the Cocos Plate. Geophys. Res. Lett. 30 (11). doi:10.1029/2002GL016766.

Gorman, A.R., Holbrook, W.S., Jornbach, M.J., Hackwith, K.L., Lizarralde, D., Pecher, I., 2002. Migration of methane gas through the hydrate stability zone in a low-flux hydrate province. Geology 30 (4), 327–330.

Grevemeyer, I., Villiner, H., 2001. Gas hydrate stability and the assessment of heat flow through continental margins. Geophys. J. Int. 145, 647–660.

Grevemeyer, I., Kopf, A.J., Fekete, N., Kaul, N., Villiner, H.W., Heesemann, M., Wallmann, K., Spiess, V., Gerrerich, H.H., Mueller, M., Weinrebe, W., 2004. Fluid flow through active mud dome Mound Culebra offfshore Nicoya Peninsula, Costa Rica: evidence from heat flow surveying. Mar. Geol. 207, 145–157.

Grevemeyer, I., Kaul, N., Diaz-Naveas, J.L., Villinger, H.W., Ranero, C.R., Reichert, C., 2005. Heat flow and bending-related faulting at subduction trenches: case studies offshore of Nicaragua and Central Chile. EPSL 236, 238–248.

Handa, Y.P., Stupin, D., 1992. Thermodynamic properties and dissociation characteristics of methane and propane hydrates in 70-Angstrom-radius silica-gel pores. J. Phys. Chem. 96, 8599–8603.

Henry, P., Le Pichon, Lallemant, S., Lance, S., Martin, J.B., Foucher, J.P., Alina, F.M, Rostek, F., Guilhaumou, N., Pranal, V., a. Castrec, M., 1996. Fluid flow in and around a mud volcano field seaward of the Barbados accretionary wedge: results from Manon cruise. J. Geophys. Res. 101 (B9), 20,297–20,323.

Hensen, C., Wallmann, K., Schmidt, M., Ranero, C.R., Hahling, H., Suess, E., 2004. Fluid expulsion related to mud volcanism at Costa Rica continental margin — a window to the subducting slab. Geology 32, 201–204.

Holbrook, W.S., Hoskins, H., Wood, W.T., Stephen, R.A., Lizarralde, D., Party, L.S., 1996. Methane hydrate and free gas on the Blake Ridge from vertical seismic profiling. Science 273 (5283), 1840–1843.

Ivanov, M.K., Limonov, A.F., Weering, T.C.E.V., 1996. Comparative characteristics of the Black Sea and Mediterranean Ridge mud volcanoes. Mar. Geol. 132, 253–271.

Jackson, M.P.A., Vendeville, B.C., 1994. Regional extension as a geologic trigger for diapirism. Geol. Soc. Amer. Bull. 106, 57–73.

Kahn, L.M., Silver, E.A., Orange, D., Kochevar, R., McAdoo, B., 1996. Surficial evidence of fluid expulsion from the Costa Rica accretionary prism. Geophys. Res. Lett. 23 (8), 887–890.

Kimura, G., Silver, E.E., Blum, P., 170, S.S.P.L., 1997. Proc. ODP, Initial reports, Ocean Drilling Program, College Station, TX.

Kopf, A., 2002. Significance of mud volcanism. Rev. Geophys. 40 (2). 1005. doi:10.1029/2000RG000093.

Kutterolf, S., Schacht, U., Freundt, A., Wehrmann, H., Moerz, T., Schmidt, M., Schmincke, H.-U., 2004. Marine Tephras offshore Nicaragua and Costa Rica — determination of sedimentation rates, eruption volumes, marine. IAVCEI Generally Assembly, Pucon.

Langseth, M.G., Silver, E.A., 1996. The Nicoya convergent margin — a region of exceptionally low heat flow. Geophys. Res. Lett. 23 (8), 891–894.

MacIntosh, K.D., Silver, E.A., Ahmed, I., Berhorst, A., Ranero, C.R., Kelly, R.K., Flueh, E., 2006. The Nicaragua Convergent Margin: seismic reflection imaging of the source of a tsunami earthquake, Costa Rica. In: Moore, J.C. (Ed.), The Seismogenic Zone of Subduction Thrust Faults. Columbia University Press, New York, pp. 257–287.

Mann, D.M., MacKenzie, A.S., 1990. Prediction of pore fluid pressures in sedimentary basins. Mar. Petrol. Geol. 7, 55–65.

Mau, S., Rehder, G., Stange, K., 2003. Water column studies. IMF-Geomar Rep. 115, 492.

McAdoo, B., Orange, D., Silver, E.A., McIntosh, K.D., Abbott, L., Galewsky, J., Kahn, L.M., Protti, M., 1996. Seafloor structural observations, Costa Rica accretionary prism. Geophys. Res. Lett. 23 (8), 883–886.

Milkov, A.V., 2000. Worldwide distribution of submarine mud volcanoes and associated gas hydrates. Mar. Geol. 167, 29–42.

Moerz, T., Fekete, N., Kopf, A., Brueckmann, W., Kreiter, S., Huehnerback, V., Masson, D., Hepp, D.A., Schmidt, M., Kutterolf, S., Sahling, H., Abegg, F., Spiess, V., Suess, E., Ranero, C.R., 2005. Style and productivity of mud diapirism along the middle American margin: Part II: Mound Culebra and Mounds 11 and 12. In: Panahi, B. (Ed.), Mud Volcanoes, Geodynamics and Seismicity. Springer, Dordrecht, The Netherlands, pp. 49–76.

Osborne, M.J.a., Swarbrick, R.E., 1997. Mechanisms for generating overpressure in sedimentary basins: a reevaluation. AAPG Bull. 81 (6), 1023–1041.

Pecher, I.A., Ranero, C.R., von Huene, R., Minshull, T.A., Singh, S.C., 1998. The nature and distribution of bottom simulation reflectors at the Costa Rican convergent margin. Geophys. J. Int. 133, 219–229.

Ranero, C.R., von Huene, R., 2000. Subduction erosion along the Middle America convergent margin. Nature 404, 748–752.

Ranero, C.R., von Huene, R., Flueh, E., 2000. A cross section of the convergent Pacific margin of Nicaragua. Tectonics 19, 335–357.

Ruppel, C., 1997. Anomalously cold temperatures observed at the base of gas hydrate stability zone on the US passive continental margin. Geology 25, 699–704.

Saffer, D.M., 2003. Pore pressure development and progressive dewatering in the underthrust sediments at the Costa Rican subduction margin: comparison with northern Bardados and Nankai. J. Geophys. Res. 108 (B5), 2261. doi:10.1029/2002JB001787.

Sahling, H., Echeverria-Saenz, S., Corrales-Cordero, E.M., Soeding, E., Suess, E., 2003. Sea Floor Observation by OFOS, vol. 115. IMF-Geomar, Kiel.

Schmidt, M., Hensen, C., Moerz, T., Mueller, C., Grevemeyer, I., Wallmann, K., Mau, S., Kaul, N., 2005. Methane hydrate accumulation in "Mound 11" mud volcano, Costa Rica forearc. Mar. Geol. 216, 83–100.

Shipley, T.H., Stoffa, P.L., Dean, D.F., 1990. Underthrust sediments, fluid migration paths, and mud volcanoes associated with the accretionary wedge off Costa Rica: Middle America Trench. J. Geophys. Res. 95 (B6), 8743–8752.

Shipley, T.H., McIntosh, K.D., Silver, E.A., Stoffa, P.L., 1992. Three dimensional seismic imaging of the Costa Rica Accretionary Prism: structural diversity in a small volume of the lower slope. J. Geophys. Res. 97 (B4), 4439–4459.

Silver, E.A., Kastner, M., Fisher, A., Morris, J., McIntosh, K.D., Saffer, D., 2000. Fluid flow path in the Middle America trench and Costa Rica margin. Geology 28, 679–682.

Talukder, A.R., Comas, M.C., Soto, J.I., 2003. Pliocene to Recent mud diapirism and related mud volcanoes in the Alboran Sea (Western Mediterranean). In: Morley, C.K. (Ed.), Subsurface Sediment Mobilization. The Geological Society, London, pp. 443–459.

Taylor, M.H., Dillon, W.P., Pecher, I., 2000. Trapping and migration of methane associated with the gas hydrate stability zone at the Blake Ridge Diapir: new insights from seismic data. Mar. Geol. 164, 79–89.

Van Rensbegen, P., Morley, C.K., Ang, D.W., Hoan, T.Q., Lam, N.T., 1999. Structural evolution of shale diapirs from reactive rise to mud volcanism: 3D seismic data from the Baram delta, offshore Brunei Darussalam. J. Geol. Soc. (Lond.) 156, 633–650.

Vendeville, B.C., Jackson, M.P.A., 1992. The rise of diapirs during thin-skinned extension. Mar. Petrol. Geol. 9, 331–353.

von Huene, R., Ranero, C.R., Watts, P., 2004. Tsunamigenic slope failure along the Middle America Trench in two tectonic settings. Mar. Geol. 203, 303–317.

Wood, W.T., Gettrust, J.F., Chapman, N.R., Spence, G.D., Hyndman, R.D., 2002. Decreased stability of methane hydrates in marine sediments owing to phase-boundary roughness. Nature 420, 656–660.

Zakrzewski, M., Handa, Y.P., 1993. Thermodynamic properties of ice and of tetrahydrofuran hydrate in confined geometries. J. Chem. Thermodyn. 25, 631–637.